Journal of Hazardous Materials 165 (2009) 589–598

Contents lists available at ScienceDirect

Journal of Hazardous Materials

journal homepage: www.elsevier.com/locate/jhazmat

Adsorption behaviour of methylene blue onto Jordanian diatomite: A kinetic study

Mohammad A. Al-Ghouti[a,*], Majeda A.M. Khraisheh[b,1], Mohammad N.M. Ahmad[c,2], Stephen Allen[c,2]

[a] Industrial Chemistry Centre, Royal Scientific Society, P.O. Box: 1438 Amman, Jordan
[b] Department of Civil and Environmental Engineering, University College London, Gower Street, London WC1E 6BT, UK
[c] School of Chemistry and Chemical Engineering, Queen's University Belfast, Stranmillis Road, Belfast BT9 5AG, UK

ARTICLE INFO

Article history:
Received 15 July 2008
Received in revised form 5 October 2008
Accepted 7 October 2008
Available online 14 October 2008

Keywords:
Adsorption
Diatomite
Methylene blue
Kinetic studies
Waste treatment

ABSTRACT

The effect of initial concentration, particle size, mass of the adsorbent, pH and agitation speed on adsorption behaviour of methylene blue (MB) onto Jordanian diatomite has been investigated. The maximum adsorption capacity, q, increased from 75 to 105 mg/g when pH of the dye solution increased from 4 to 11. It is clear that the ionisable charge sites on the diatomite surface increased when pH increased from 4 to 11. When the solution pH was above the pH_{ZPC}, the diatomite surface had a negative charge, while at low pH (pH < 5.4) it has a positive charge. The adsorption capacity increased from 88.6 to 143.3 mg/g as the initial MB concentrations increased from 89.6 to 225.2 mg/dm^3. The experimental results were also applied to the pseudo-first and -second order kinetic models. It is noticed that the whole experimental data of MB adsorption onto diatomite did not follow the pseudo-first order model and had low correlation coefficients (R^2 < 0.3). The calculated adsorption capacity, $q_{e,cal}$, values obtained from pseudo-first order kinetic model did not give acceptable values, $q_{e,exp.}$

The maximum uptake capacity seems to be independent of the particle size of the diatomite when the particle size distribution is less than 250–500 μm. While at larger particle size 250–500 μm, the maximum uptake capacity was dependent on the particle size. It would imply that the MB adsorption is limited by the external surface and that intraparticle diffusion is reduced. The effect of the agitation speeds on the removal of MB from aqueous solution using the diatomite is quite low. The MB removal increased from 43 to 100% when mass of the diatomite increased from 0.3 to 1.7 g.

1. Introduction

The removal of coloured and colourless organic pollutants from industrial wastewater is considered an important application of adsorption processes using a suitable adsorbent [1]. There is growing interest in using low cost, commercially available materials for the adsorption of dyes. Diatomite, a siliceous sedimentary rock available in abundance in various locations around the world, has received attention for its unique combination of physical and chemical properties (such as high permeability, high porosity, small particle size, large surface area, low thermal conductivity and chemical inertness) and as low cost material for the removal of pollutants from wastewater [2]. For a successful scale-up of such a process, kinetic studies are essential since they describe the adsorbate uptake rate, which in turn controls the residence time in the adsorbent–solution interface. Many factors could affect the adsorption rate of MB adsorption onto Jordanian diatomite. In this study, initial dye concentration, particle size, mass of the adsorbent, pH and agitation speed were investigated and the results were analysed using different kinetic models.

Various kinetic models have been reported in the literature to describe the adsorption process [3,4]. Each model has its own limitations and is derived according to certain conditions. In this paper, three kinetic adsorption models will be used to describe the experimental data.

The pseudo-first order equation could be described as [3],

$$\log(q_e - q_t) = \log(q_e) - \frac{k_1}{2.303}t \Rightarrow \ln(q_e - q_t) = \ln(q_e) - k_1 t \quad (1)$$

By rearranging,

$$\ln\left(\frac{q_e - q_t}{q_e}\right) = -k_1 t \Rightarrow q_t = q_e(1 - \mathrm{Exp}(-k_1 t)) \quad (2)$$

* Corresponding author. Tel.: +96265344701; fax: +96265344806.
E-mail addresses: mghouti@rss.gov.jo, ghoutijo@yahoo.co.uk (M.A. Al-Ghouti), m.khraisheh@ucl.ac.uk (M.A.M. Khraisheh), mnm.ahmad@qub.ac.uk (M.N.M. Ahmad), s.allen@qub.ac.uk (S. Allen).
[1] Tel.: +44 20 7679 7994.
[2] Tel.: +44 28 9097 4389; fax: +44 28 9097 4627.

0304-3894/$ – see front matter © 2008 Elsevier B.V. All rights reserved.
doi:10.1016/j.jhazmat.2008.10.018

where q_t is the amount of solute adsorbed on the surface of adsorbent (mg/g) at any time t (min), q_e is the amount of MB adsorbed at equilibrium (mg/g).

To calculate the rate constant of pseudo-first order, k_1, a plot of $\ln(q_e - q_t)$ versus t gives a straight line with slope equals to $(-k_1)$. In many cases the value of q_e is unknown and adsorption tends to become unmeasurably slow. Thus, it is necessary to obtain the real equilibrium adsorption capacity by extrapolating the experimental data to $t = \infty$ or by using a trial and error method [5].

However, the simplest way to describe the kinetics of MB removal from an aqueous solution could be represented by using a pseudo-second order equation [6]

$$\frac{t}{q_t} = \frac{1}{h} + \frac{1}{q_e}t, \quad h = k_2 q_e^2 \\ \Rightarrow q_t = q_e \frac{q_e k_2 t}{1 + q_e k_2 t}, \tag{3}$$

k_2 is the rate constant of a pseudo-second order equation (g/mg min) and h is the initial adsorption rate (mg/g min).

In the intraparticle diffusion model, the relationship between q_t and $t_{1/2}$ could be written as [7],

$$q_t = x_i + k_p t^{1/2}, \tag{4}$$

where k_p is the intraparticle diffusion constant (mg/g $\text{min}^{1/2}$)and x_i is the intercept of the line which is proportional to the boundary layer thickness.

The intraparticle diffusion coefficient, D, was determined by using the following equations, which are derived from Fick's law [8,9],

$$F(t) = \frac{C_0 - C_t}{C_0 - C_e} = \frac{q_t}{q_e} = \left[1 - \exp\left(-\frac{\pi^2 D t}{r^2}\right)\right]^{1/2}$$

or

$$\ln[1 - F(t)^2] = -\frac{\pi^2 D}{r^2}t, \tag{5}$$

where C_0 is the initial MB concentration (mg/dm^3), C_t is the MB concentration (mg/dm^3) at time t (min), C_e is the MB equilibrium concentration (mg/dm^3), D is the intraparticle diffusion coefficient (m^2/s) and r is the particle radius assuming spherical geometry (m).

A plot of $\ln[1 - F(t)^2]$ versus time, t, should be linear with a slop of $-\pi^2 D/r^2$, which is commonly known as the diffusional rate constant.

However, in the early stages of contact (between 0 and 5 min of contact) the system can be simplified by assuming that the concentration at the adsorbent surface tends toward zero (i.e., pure external diffusion and the intraparticle diffusion to be negligible). Thus, the external diffusion process could be treated as follows:

$$\left[\frac{d(C_t/C_0)}{dt}\right]_{t=0} = -k_f \frac{A}{V} \Rightarrow \\ \ln\frac{C_t}{C_0} = -k_f \frac{A}{V}t = -k_f\left(\frac{6m}{d_m \rho}\right)t \\ \Rightarrow q_t = \left(\frac{V}{m}C_0\right)\left[1 - \text{Exp}\left(-k_f \frac{A}{V}t\right)\right] \tag{6}$$

where C_0 is the initial MB concentration (mg/dm^3), C_t is the MB concentration at time t (min), k_f is the external surface diffusion coefficient (m/min), A is the external surface area of the diatomite (m^2/g), V is the volume of solution (dm^3), m is the mass of the diatomite (g/dm^3), d_m is the mean particle diameter (m) and ρ is the density of the diatomite (g/dm^3) (diatomite density = 1.74 g/cm^3 = 1.74×10^3 g/dm^3).

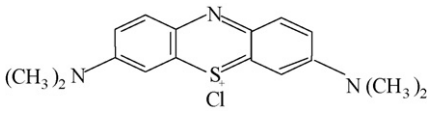

Fig. 1. The molecular structure of MB.

2. Experimental materials and methods

Methylene blue (MB) was selected as a model dye system. MB represented a basic-dye system with well-known properties (Basic-dye 9(C.I. 52015), Solid, λ_{max}: 663 nm, ε: 170.1 $\text{dm}^3\,\text{g}^{-1}\,\text{cm}^{-1}$) and its chemical structure is illustrated in Fig. 1.

2.1. Adsorbent

Diatomite samples were obtained from borehole BT-36, depth 34–36 m in Al-Azraq region in East Jordan. Quantitative chemical analysis of the diatomite obtained by X-ray florescence (XRF) technique revealed that the Jordanian diatomite consists mainly of SiO_2 (72%), and it has 11.42% Al_2O_3, 5.81% Fe_2O_3, 7.21% Na_2O and 1.48% CaO. Before use, the diatomite was washed several times with deionised water and dried overnight in an oven at 100 °C and then allowed to cool in a desiccator. Other physical characteristics have been reported in the previous publications [2,6].

2.2. Kinetic studies

The MB solution to be treated and the diatomite were agitated in a beaker for a sufficient period of time to enable the system to approach equilibrium. Kinetic studies were carried out in a 2 dm^3 glass beaker. The glass beaker was equipped with four plastic baffles distributed around the circumference. A six stainless steel flat blade impeller using an electric motor (Heidolph, RZR1) stirred the MB solution. Fig. 2 illustrates the schematic diagram of batch reactor.

The adsorbent particles were thoroughly mixed with 1.7 dm^3 of the MB solution in the beaker at constant temperature 22 °C. Just prior to adding the adsorbent material to the beaker, four milliliters were taken from the beaker to calculate the initial MB concentration. Four milliliters samples were withdrawn at different time

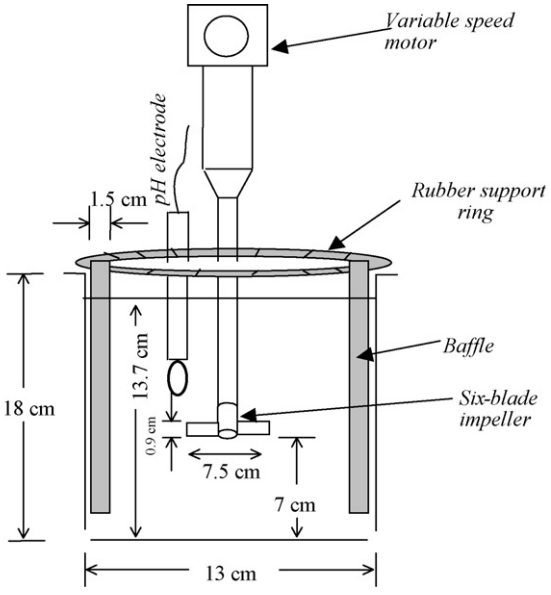

Fig. 2. Schematic diagram of the batch reactor used in this study.

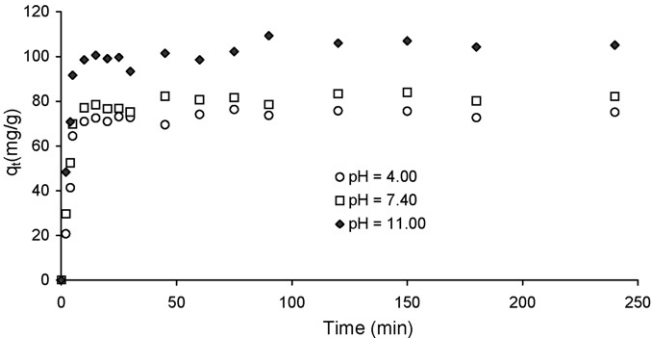

Fig. 3. The effect of pH of MB solution on the removal of MB from aqueous solution by diatomite. Experimental conditions: Initial MB concentration: 100 mg/dm^3, mass of diatomite: 1.0 g, particle size: 106–250 μm, agitation speed: 300 rpm, and temperature: 22 °C.

intervals over 360 min and put it in different cuvettes for settling. Different time intervals were chosen: 0, 5, 10, 15, 20, 25, 30, 60, 90, 120, 150, 180, 240, 300 and 360 min. This small sample volume ensures that the volume of MB solution remains constant throughout the experiment. The final MB concentrations were determined using a PerkinElmer UV–vis spectrophotometer corresponding to λ_{max} of MB dye. The amount of MB adsorbed, q_t, at time t was calculated from the following equation,

$$q_t = \frac{(C_0 - C_t)V}{m} \quad (7)$$

where C_0 (mg/dm^3) is the initial MB concentration, C_t (mg/dm^3) is the concentration of MB at time, t (min), V (dm^3) is the volume of MB solution and m is the mass of adsorbent.

The effect of initial MB concentration, particle size, pH, mass of adsorbent on MB adsorption was studied and the experimental conditions are illustrated in Table 1. After the equilibrium time of 360 min, the absorbance of MB in the equilibrium solution was determined.

3. Results and discussion

3.1. Effect of pH

The concentration of hydrogen and hydroxyl ions affects the adsorption process through the dissociation of functional groups on the diatomite surface. The effect of solution pH on MB adsorption onto diatomite was studied and the results are illustrated in Fig. 3. It indicates that the adsorption rate of MB adsorption onto diatomite is very fast at the early stages (0–5 min) and then slows down gradually.

It seems from Fig. 3 that the adsorption capacity of MB onto diatomite increased with the increase in pH. The maximum adsorption capacity, q, increased from 75 to 105 mg/g when pH of the dye solution increased from 4 to 11. It was shown that the zero point of charge, pH_{ZPC}, of the diatomite was 5.4 [2]. Thus, it is clear that the ionisable charge sites on the diatomite surface increased when pH increased from 4 to 11. When the solution pH was above the pH_{ZPC}, the diatomite surface had a negative charge, while at low pH (pH < 5.4) it has a positive charge. Hence, when the pH of MB solution increased, the association of MB molecules increased as described in Eqs. (8) and (9),

$$Si{-}OH + {}^{-}OH \rightleftharpoons Si{-}O^{-} + H_2O \quad (8)$$

$$Si{-}O^{-} + MB^{+} \rightleftharpoons Si{-}O^{-+}MB \quad (9)$$

From Fig. 3, it can be seen that the shape of q_t versus time plots of MB adsorption onto diatomite at pH 4 and 7.4 are quite similar in comparison to that at pH 11. This might be due to the high negative surface charge density on the diatomite surface at pH 11. Al-Ghouti et al. [2] reported that the surface charge density of the diatomite at pH 4, 7.4 and 11 were +0.136, −0.06 and < −0.22 C/m^2, respectively.

3.2. Effect of initial MB concentration

Several experiments were carried out to determine the effect of initial MB concentration on the MB removal kinetics from aqueous solution. However, initial concentration provides an important driving force to overcome all the mass transfer resistance of MB between the aqueous solution and the diatomite surface. As a result, high initial MB concentration will enhance the adsorption process [5]. Adsorption kinetic studies were measured as a function of initial dye concentration and the results are illustrated in Fig. 4. Here, the fraction of MB in the solution was defined as the ratio of MB concentration in the solution at time t, C_t, to the initial MB concentration, C_0. The adsorption capacity increased from 88.6 to 143.3 mg/g as the initial MB concentrations increased from 89.6 to 225.2 mg/dm^3.

Fig. 4 indicates that the adsorption of MB was very fast in the first few minutes (0–5 min). It is found that the time required to reach the adsorption equilibrium between the diatomite and MB solution was less than 45 min. The dye concentration decreased in the first contact of the diatomite with MB, where the concentration of MB decreased to 16, 34, 45 and 49% from the initial dye concentration in the first five minutes when the MB concentration was 89.6, 149.6, 211.98 and 255.21 mg/dm^3, respectively (see Fig. 4). Steep slope curves of MB adsorption onto diatomite indicate instantaneous adsorption which may be due to effects of surface acidic functional groups (silanol groups Si–OH) found on the diatomite surface. Therefore, the adsorption of MB is thought to have taken place probably via surface adsorption until the surface functional sites are fully occupied, thereafter, MB molecules diffuse into the pores of the diatomite for further adsorption. The same behaviour was observed by Mohan and Singh [10].

Due to the porosity of the diatomite, intraparticle diffusion was expected in the adsorption process. This was examined by plotting MB uptake, q_t, against the square root of time, $t^{0.5}$, as shown in Fig. 5. It is clear that the curves in Figs. 4 and 5 represent three distinct phases: (i) instantaneous adsorption of MB molecules within 5 min of the contact times, (ii) a gradual attainment of the equilibrium where only about 2–8% of the adsorption is encountered. This is due to the utilisation of the all active sites on the adsorbent

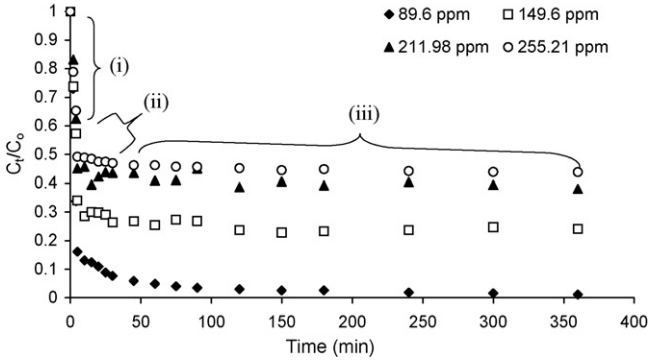

Fig. 4. The effect initial dye concentrations on MB adsorption onto diatomite. Experimental conditions: mass of diatomite: 1.7 g, volume of dye solution: 1.7 dm^3, particle size: 250–500 μm, agitation speed: 300 rpm, pH: 11, and temperature: 22 °C ((i) instantaneous adsorption of MB molecules within 5 min of the contact times, (ii) a gradual attainment of the equilibrium where only about 2–8% of the adsorption is encountered, and (iii) an equilibrium attainment of MB molecules onto diatomite).

Table 1
Experimental conditions of the various kinetic adsorption experiments for the removal of MB onto diatomite at constant volume of dye solution (1.7 dm^3).

Parameter	pH	Mass of adsorbent (g)	Particle size (μm)	Initial dye concentration (mg/dm^3)	Agitation speed (rpm)
pH	4, 7.4, 11	1.0	(106–250)	100	300
Mass of adsorbent (g)	11	1.7, 1, 0.7, 0.3	(106–250)	100	300
Particle size (μm)	11	1.7	(<106), (106–250), (250–500)	100	300
Initial dye concentration (mg/dm^3)	11	1.7	(250–500)	100, 150, 200, 250	300
Agitation speed (rpm)	11	1.7	(250–500)	100	200, 300, 400

surface and (iii) an equilibrium attainment of MB molecules onto diatomite. In addition, the initial curves are linear and the final portion is also linear. The initial curved portions may be attributed to the boundary layer diffusion effect, while the final linear portions are related to the intraparticle diffusion effects. Mohan and Singh [10] observed the same behaviour of adsorption of azo dyes onto coal-based sorbents. Thus, the slope of a linear portion is related to the intraparticle diffusion parameter, k_p, and is characteristic of the rate of adsorption in this region where intraparticle diffusion is the rate-limiting step [10]. The intraparticle diffusion parameter, k_p, is defined as the linear gradient for the relationship of the amount of dye adsorbed per gram of adsorbent at time t. Although this rate parameter does not have the usual dimension of a rate parameter, it has similar characteristics to the rate of an adsorption process over the linear portion of the plot [11]. However, the experimental data at various initial MB concentrations were applied to the intraparticle diffusion kinetic model and the results are illustrated in Table 2. It is observed that the straight line of the intraparticle region did not pass through the origin and indicates that the intraparticle diffusion is not the only rate-limiting step [10].

The experimental results were also applied to the pseudo-first and -second order kinetic models. It is noticed that the whole experimental data of MB adsorption onto diatomite did not follow the pseudo-first order model and had low correlation coefficients ($R^2 < 0.3$). The calculated adsorption capacity, $q_{e,cal}$, values obtained from pseudo-first order kinetic model did not give acceptable values, $q_{e,exp}$ [2]. Fig. 6 shows that multiple lines are presented. Basically, a multiple pseudo-first order process means that a plot of $\log(q_e - q_t)$ versus time, t, can be divided into two or three linear sections, each linear section representing a pseudo-first order reaction mechanism. One stage corresponds to the initial binding of the adsorbate molecules with the active sites on the adsorbent surface, and the other stages represent a tendency of the adsorbate to form a uniform layer on the surface of the adsorbent [3,12]. It seems from Fig. 6 that the adsorption during the first step is very rapid compared with other stages, which are controlled by a film or intraparticle diffusion mechanism. The $q_{e,cal}$ values agreed with the experimental values, $q_{e,exp}$, in the case of pseudo-second order kinetic model especially at low dye concentrations. When the experimental results were applied to the pseudo-second order model, straight lines with high correlation coefficients ($R^2 = 0.9998$) were obtained indicating that the adsorption process applies to the pseudo-second order kinetic model and the results are illustrated in Table 2.

A comparison of pseudo-first and -second order kinetic models of MB adsorption onto diatomite at various initial dye concentrations are illustrated in Fig. 7. This shows that pseudo-second order model is most applicable in describing MB adsorption onto diatomite.

Table 2 shows that the intraparticle parameter, k_p, increases with initial MB concentration increases from 89.6 to 149.6 and from 212 to 255 mg/dm^3. This could be attributed to the driving force of diffusion. The driving force changes with the dye concentration in the bulk solution. Thus, the increase of MB concentration results

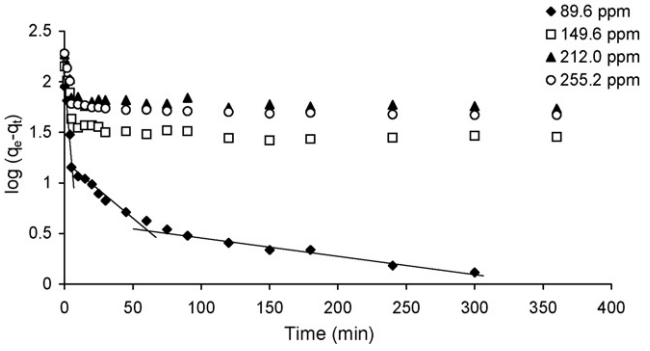

Fig. 6. Pseudo-first order adsorption kinetics of MB onto diatomite at various initial dye concentrations. Experimental conditions: mass of diatomite: 1.7 g, volume of solution: 1.7 dm^3, pH: 11, particle size: 250–500 μm, agitation speed: 300, and temperature: 22 °C.

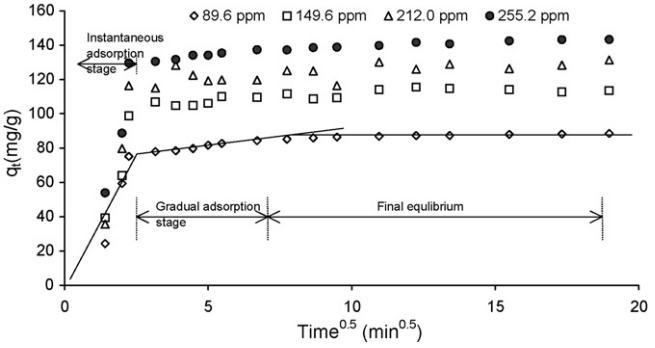

Fig. 5. Three stages of MB adsorption onto diatomite and intraparticle diffusion plot of adsorption of MB onto diatomite at various initial MB concentrations. Experimental conditions: mass of diatomite: 1.7 g, particle size: 250–500 μm, agitation speed: 300 rpm, pH: 11, and temperature: 22 °C.

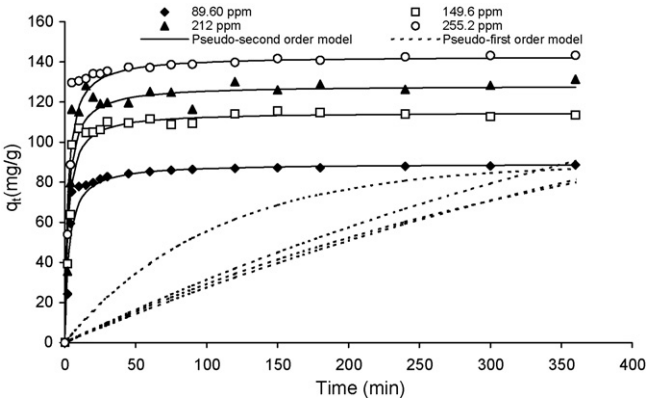

Fig. 7. A comparison of pseudo-first and -second order kinetic models of MB adsorption onto diatomite at various initial dye concentrations. Experimental conditions: mass of diatomite: 1.7 g, volume of solution: 1.7 dm^3, pH: 11, particle size: 250–500 μm, rotating speed: 300, and temperature: 22 °C.

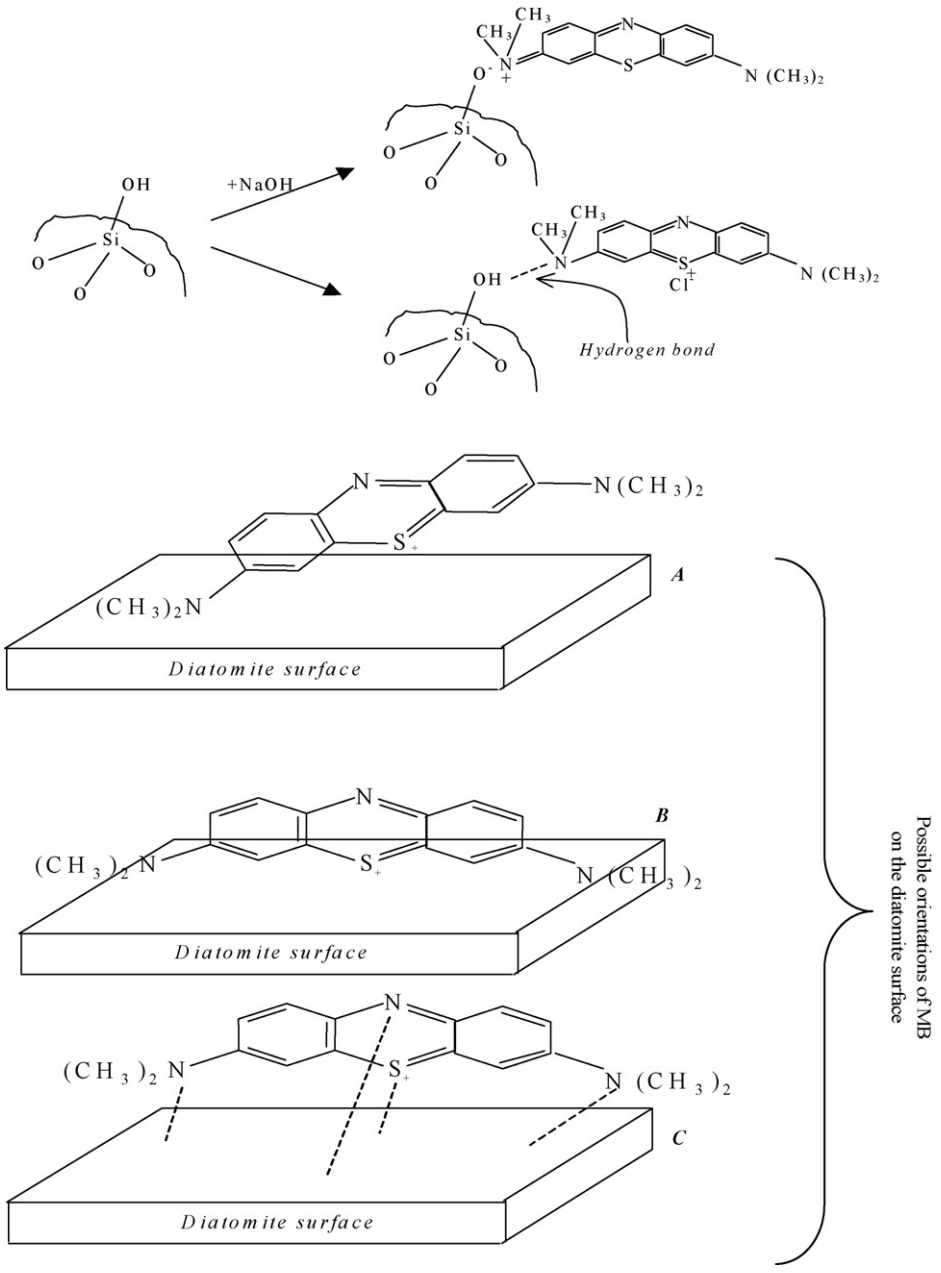

Fig. 8. Proposed mechanism of MB adsorption on diatomite surface and the possible orientations of MB on the diatomite surface.

in an increase in the driving force, which will increase the diffusion rate of the molecular dye in pores. However, Table 2 also shows that the effect of initial MB on the intraparticle diffusion parameter, k_p, was low and irregular. This suggests that the rate-limiting step of MB adsorption onto diatomite is represented by external diffusion instead of transport phenomena inside solid particle. The irregularity of the k_p could be related to the heterogeneity of the diatomite structure and the capability of MB molecules to agglomerate on its surface, especially at high dye concentrations. Al-Ghouti et al. [2] showed explicitly the adsorption mechanism of MB molecules onto the diatomite surface. In addition, Fig. 8 shows a schematic representation of MB adsorption onto diatomite surface. Moreover, the MB agglomeration might cause blockage of the pores on the diatomite structure [13,14]. However, the intraparticle diffusion plots with high correlation coefficients indicate the presence of the intraparticle diffusion process as one of the rate-limiting steps in the adsorption system of MB onto diatomite. Moreover, it is clear from Fig. 5 that the straight lines of the intraparticle plots do not pass through the origin and the values of x_i, which relates to the boundary layer resistance, is relatively high, i.e., the larger the intercept, x_i, the greater is the contribution of the surface adsorption in the rate-limiting step; hence, the intraparticle diffusion process may not be the sole rate-limiting step in the adsorption process (Ho and McKay [12]). Table 2 illustrates that the intraparticle diffusion coefficient, D, decreases with increasing initial dye concentration. It could also be explained by the capability of the dye to form micelles (aggregation behaviour) at high concentrations [14]. For pore diffusion, the rate of pore diffusion, D, should be in the range between 10^{-11} and 10^{-13} cm^2/s. Moreover, the value of intraparticle diffusion coefficient, D, at various initial dye concentrations was between 3×10^{-8} and 9×10^{-8} cm^2/s. This shows that the D value is high, suggesting that the intraparticle diffusion process is

Table 2
Intraparticle, external diffusion, pseudo-first and -second order kinetic parameters of MB adsorption onto diatomite at various initial MB concentrations.

Conc. (mg/dm^3)	Pseudo-first order			Pseudo-second order			Intraparticle diffusion		External diffusion	Intraparticle diffusion		
	$q_{e,exp}$ (mg/g)	$q_{e,cal}$ (mg/g)	k_1 (1/min)	$q_{e,cal}$ (mg/g)	k_2 (g/mg min)	h (mg/g min)	k_p (mg/g min$^{1/2}$)	x_i	k_f (m/min)	k' (1/min)	D (cm^2/s)	R^2
89.60	89.45	14.98	0.0097	89.29	0.0039	31.09	2.24	70.22	0.038	0.1596	9.45×10^{-8}	0.8898
149.6	141.9	47.34	0.0023	114.9	0.0038	50.51	2.51	95.14	0.021	0.0911	5.41×10^{-8}	0.8627
212.0	185.7	81.28	0.0016	128.2	0.0034	55.87	1.30	114.9	0.017	0.0543	3.22×10^{-8}	0.7394
255.2	190.1	72.11	0.0018	142.9	0.0032	65.31	1.87	125.1	0.014	0.0698	4.14×10^{-8}	0.7731

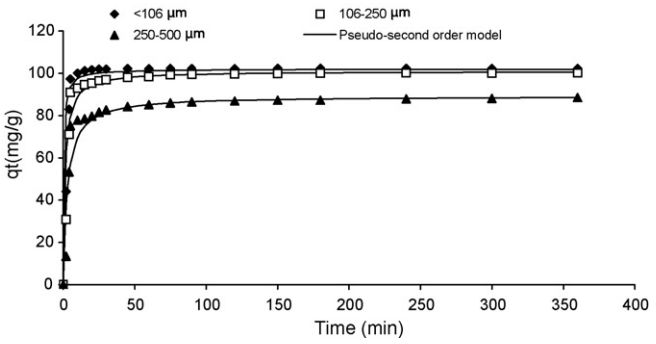

Fig. 9. Effect of diatomite particle size on MB adsorption. Experimental conditions: mass of diatomite: 1.7 g, pH of solution: 11.0, volume of solution: 1.7 dm^3, temperature: 21 °C, agitation speed: 300 rpm, and initial dye concentration: 100 mg/dm^3.

not the only rate-limiting step in MB adsorption onto diatomite. Thus, the intraparticle diffusion may have a little effect on MB adsorption onto diatomite. Moreover, the film diffusion coefficient is relatively more important than pore diffusion in MB adsorption. It is shown in Table 2 that the values of external diffusion coefficient, k_f, decrease by increasing initial dye concentration. Khraisheh et al. [15] reported the effect of surface area and pore distribution on MB adsorption onto diatomite. They showed that mesopores are dominant of the total pore volume for diatomite and calcined diatomite. The contribution of macropores in adsorption is less than 1% of the total surface area. The mesopores have the most influence in the adsorption of organic solutes, which enables their surfaces to be accessible to solute molecules.

The rate coefficient of the pseudo-second order kinetic model decreased from 3.9×10^{-3} to 3.2×10^{-3} mg/g min when the initial MB concentration increased from 89.6 to 255.2 mg/dm^3. The kinetic parameters of MB adsorption onto diatomite were calculated from the slope and the intercept of the linearised form of the pseudo-second order equation. It seems from Table 2 that the values of h increase with the increase in the initial MB concentration. The value of h increased from 31.09 to 65.31 mg/g min. This behaviour was observed by various authors [16,17]. This could be attributed to many factors; increasing the dye concentration might reduce the diffusion of dye molecules in the boundary layer and enhance the diffusion in the solid. Chu [17] also explained this behavior in terms of the degree of adsorbate loading on the adsorbent. At low initial concentration, the adsorbate will bind preferentially to high-energy sites because they are usually taken up by the adsorbent first and then sites of lower energy are progressively filled as the adsorbate loading is increased. Therefore, the higher value of rate parameter of pseudo-second order is to be expected. On the other hand, high initial dye concentration will yield a lower value of rate parameter. Moreover, increasing the MB concentration seems to decrease an electrostatic interaction of the site with lower affinity for MB molecules. It seems that the value of adsorption capacity, q_e, increased with an increased of initial dye concentration. This is due to the efficient utilisation of the adsorptive capacities of the diatomite by the greater driving force by a higher concentration gradient.

3.3. Effect of particle size

To illustrate the effect of the diatomite particle size on MB adsorption, three ranges of the particle size distribution, <106, 106–250 and 250–500 μm, were used and the results are shown in Fig. 9. It can be seen from Fig. 9 that the maximum uptake capacity seems to be independent of the particle size of the diatomite when the particle size distribution is less than 250–500 μm. While

at larger particle size 250–500 μm, the maximum uptake capacity was dependent on the particle size. It would imply that the MB adsorption is limited by the external surface and that intraparticle diffusion is reduced. Similar results were obtained on vanadium(IV) adsorption onto chitosan [18]. It was noticed that the difference between <120 and 120–250 μm on vanadium(IV) adsorption was hardly visible, but for higher particle ranges, the variation cannot be neglected. Thus, it appears that the particle size of the diatomite has a weak effect on the shape of the experimental curves except for the large particle size. However, in order to investigate the effect of the various particle sizes on MB adsorption, intraparticle diffusion, pseudo-first and -second order kinetic models were applied on the experimental data and the results are illustrated in Table 3.

It is worth noting that to examine the intraparticle diffusion as a rate-limiting step, a plot of the intraparticle diffusion parameter, k_p, versus the square of the inverse particle diameter should yield a straight line [19,20]. Theoretically, the k_p and the adsorption capacity are related to available adsorbent surface area. For a spherical adsorbent particle and for a given mass of adsorbent, the total surface area is inversely proportional to the adsorbent particle diameter. Therefore, if only surface adsorption sites were utilised for dye removal, adsorption capacity should be proportional to the inverse particle diameter, $1/d$, for a given adsorbent mass [19,20]. The plot of rate parameter versus square inverse diameter did not give a straight line and the only conclusion is that the intraparticle diffusion was not the only operative mechanism.

An examination of the effect of MB concentration on the rate parameter, k_p, provides additional information regarding to the dye adsorption process. The nature of the rate-limiting step was also confirmed by plotting the rate parameter, k_p, versus the first power of the initial concentration for the process. The rate parameter, k_p, should be proportional to the first power of concentration for the process controlled by external diffusion. However, when pore diffusion limits the adsorption process, the relationship between dye concentrations and the rate parameter, k_p, will not be linear [21]. The calculated rate parameter, k_p, was proportional to the first power of concentration only during the first 5 min of the process. This indicates that only during the initial stage of the process (0–5 min) is the adsorption controlled by external diffusion, and then the intraparticle diffusion becomes the rate-limiting step of the process [21].

Table 3 also shows that the intraparticle diffusion coefficient, D, increases with particle size. This behaviour is expected due to the decrease in the surface area available for adsorption with larger particle size. Consequently, the number of available site for adsorption reduced, the dye molecules then tend to adsorb on the surface and diffuse into the particle more readily [14]. Furthermore, the high value of the intraparticle diffusion coefficient, D, of the adsorption system at various particle size distributions indicates that the intraparticle diffusion is not the only rate-limiting step.

In addition, the variation of the particle size affects the time required to reach equilibrium in which the equilibrium time increased from 20 to 45 min as particle size increased from <106 to 250–500 μm. Thus, the decreasing particle size decreases the time required to reach equilibrium. It is clear that increasing the particle size diameter results in an increase in the external diffusion coefficient, k_f. The same trend was obtained by McKay et al. [22]. However, the smaller particle sizes agitated in a beaker will tend to follow the vortex, which was developed as the result of agitation. As a result, less shear exists between the single particle and the surrounding liquid. This behaviour is different for a large particle size in which the large particle size tend to resist motion due to its own moment of inertia and therefore relatively more shear will exist between larger particles and the liquid. Moreover, it might be explained by the fact that for a small particle a large external

Table 3
Intraparticle, diffusion, pseudo-first and -second order kinetic parameters of MB adsorption onto diatomite at various particle sizes.

Particle size (μm)	Pseudo-first order			Pseudo-second order			Intraparticle diffusion		External diffusion	Intraparticle diffusion		
	$q_{e,exp}$ (mg/g)	$q_{e,cal}$ (mg/g)	k_1 (1/min)	$q_{e,cal}$ (mg/g)	k_2 (g/mg min)	h (mg/g min)	k_p (mg/g min$^{1/2}$)	x_i	k_f (m/min)	k' (1/min)	D (cm^2/s)	R^2
<106	102.8	3.24	0.0088	102.0	0.0213	221.8	2.41	92.11	0.008	0.3234	3.84×10^{-9}	0.8145
106–250	101.1	9.87	0.0097	101.0	0.0072	73.46	1.98	86.71	0.022	0.2084	2.79×10^{-8}	0.8185
250–500	89.45	14.98	0.0097	89.29	0.0039	31.09	2.24	70.22	0.038	0.1596	9.45×10^{-8}	0.8898

Table 4
Intraparticle, external diffusion, pseudo-first and -second order kinetic parameters of MB adsorption onto diatomite at various agitation speeds.

Agitation speed (rpm)	Pseudo-first order (Whole experimental data)			Pseudo-second order (Whole experimental data)			Intraparticle diffusion		External diffusion	Intraparticle diffusion		
	$q_{e,exp}$ (mg/g)	$q_{e,cal}$ (mg/g)	k_1 (1/min)	$q_{e,cal}$ (mg/g)	k_2 (g/mg min)	h (mg/g min)	k_p (mg/g min$^{1/2}$)	x_i	k_f (m/min)	k' (1/min)	D (cm^2/s)	R^2
200	86.81	17.37	0.0083	86.21	0.0025	18.25	4.13	57.13	0.029	0.1162	6.90×10^{-8}	0.8591
300	89.45	14.98	0.0097	89.29	0.0039	31.09	2.24	70.22	0.038	0.1596	9.45×10^{-8}	0.8898
400	89.37	12.58	0.0088	88.50	0.0053	41.32	1.36	75.09	0.044	0.1719	1.05×10^{-7}	0.8937

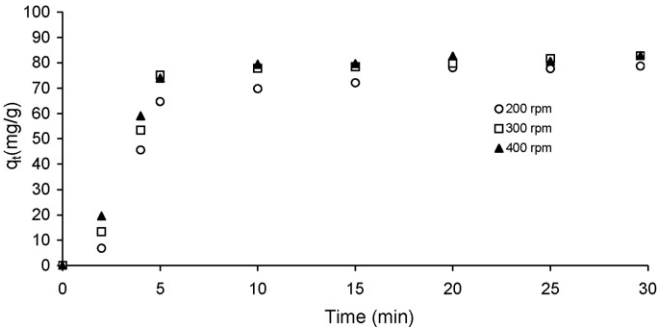

Fig. 10. Effect of agitation speeds on MB adsorption onto diatomite during the first 30 min. Experimental conditions: particle size: 250–500 μm, pH of solution: 11.0, volume of solution: 1.7 L, mass of diatomite: 1.7 g, and initial dye concentration: 100 mg/dm^3.

surface area is presented to the solute molecules and as a result lowering the driving force per unit surface area for mass transfer than for larger particles [22].

It is also noticed from Table 3 that the pseudo-second order parameter, k_2, notably decreases from 0.0213 to 0.0039 (g/mg min) as the particle size increases from <106 to 250–500 μm. It can also be shown from Table 3 that the initial rate, h and the adsorption capacity, q_e, increases with a decrease in particle size of the diatomite. This could be attributed to the mechanism of MB adsorption onto diatomite, which may be by surface adsorption. Because the adsorption of MB may govern by surface adsorption onto diatomite, it seems that the k_2 noticeably increased from 0.0039 to 0.0213 g/mg min. It is worth noting here that the $q_{e,cal}$ values agreed very well with the $q_{e,exp}$ values in the case of the pseudo-second order kinetic model. It suggests that the adsorption process of MB adsorption onto diatomite may be a pseudo-second order reaction.

3.4. Effect of agitation speed

Agitation speed influences in the distribution of the dye molecules in the bulk solution but can also act on the formation of the external boundary film [18]. The varying of the agitation speed in a batch reactor is usually used to confirm the absence of significant external resistance. If mass transfer of dye molecules is an important factor in controlling the rate, then the rate of agitation would have an effect on the uptake. Increasing agitation speed decreases the film resistance to mass transfer surrounding the adsorbent particle and increases the mobility of the system [23]. The effect of the agitation speeds on MB adsorption onto diatomite was carried out. Three agitation speeds 200, 300 and 400 rpm were tested in order to investigate the kinetic process of MB adsorption and the results are illustrated in Fig. 10. It is clear from Fig. 10 that the effect of the agitation speeds on the removal of MB from aqueous solution using the diatomite is quite low. Table 4 illustrates the pseudo-first and -second order, external and intraparticle diffusion kinetic models at various agitation speeds.

The effect of agitation speed on the intraparticle diffusion parameter was changeable. It is clear that the intraparticle parameter increased from 1.36 to 4.13 mg/g min$^{1/2}$ with decreasing the agitation speed from 400 to 200 rpm. This was probably because the resistance of the particle surface of the diatomite was low for the molecular dye from bulk solution into particle pores. Moreover, the external diffusion parameter, k_f, also increased from 0.029 to 0.044 m/min. It can be seen that there is an obvious effect of the agitation speed on the adsorption rate of MB removal by diatomite. It can be attributed to the decrease in boundary layer thickness

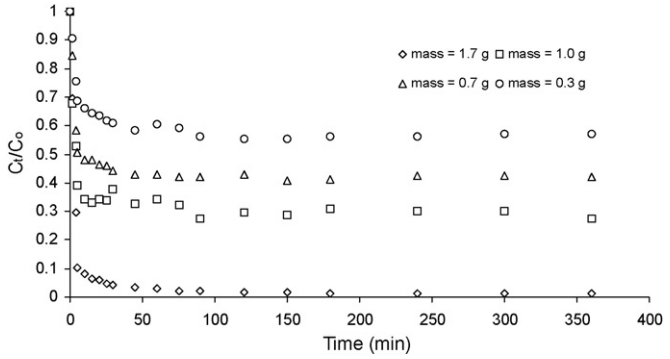

Fig. 11. Effect of mass of diatomite on MB adsorption. Experimental conditions: particle size 106–250 μm, pH of solution: 11.0, volume of solution: 1.7 dm^3, agitation speed: 300 rpm, and initial dye concentration: 100 mg/dm^3.

around the diatomite particles being a result of increasing the degree of mixing (i.e., the boundary layer resistance decreases, creating a small difference between the solute concentration in the bulk solution and at the surface of the particle) [1,24]. This indicates that the external diffusion control process may play an important role in the dye removal. A plot of $\ln(k_f)$ versus $\ln(\text{rpm})$ (rpm: agitation speed) is expected to be linear (Walker et al. [13]). This behaviour is described by Eq. (10) ($R^2 = 0.9948$),

$$\ln(k_f) = 0.61\ln(rpm) - 6.7426$$
$$\Rightarrow k_f = 1.18 \times 10^{-3}(rpm)^{0.61} \quad (10)$$

3.5. Effect of mass of diatomite

Different masses of diatomite were chosen to study the effect of the adsorbent mass on the adsorption process. 1.7, 1.0, 0.7 and 0.3 g were chosen and the experimental results are shown in Fig. 11. The concentration decays plots of MB adsorption at various masses of adsorbent onto diatomite are illustrated in terms of the ratio of C_t/C_0 versus time, t. It can be seen that the MB removal increased from 43 to 100% when mass of the diatomite increased from 0.3 to 1.7 g. Different kinetic models were also used to calculate the adsorption parameters at various masses of adsorbent and the results are shown in Table 5.

It is known that the diatomite surface contains silanol groups, which could act as active centres for exchange with cationic basic-dye (MB), and thus leading to the chemical adsorption mechanism. The value of intraparticle diffusion parameter, k_p, remarkably increased from 1.98 to 12.76 $mg/g\,min^{1/2}$ when mass of the diatomite decreased from 1.7 to 0.3 g. Thus, resistance due to intraparticle diffusion could be considered as negligible when the high adsorbent masses were used. When the adsorbent mass increased, the ratio of adsorbent/adsorbate in the system increased, resulting in the domination of external diffusion and reduced the effect of intraparticle diffusion [22]. In addition, it is shown from Table 5 that the $q_{e,cal}$ values of pseudo-second order equation do not agree well with the experimental values, $q_{e,exp}$ when the mass of the diatomite was less than 1.7 g.

It is observed from Table 5 that increasing the mass of the diatomite results in an increase in the external diffusion parameter, k_f. This behaviour could be explained as the external mass transfer coefficient will depend on the driving force per unit area. Consequently, increasing the mass of the diatomite increases the surface area for adsorption and hence the rate of MB removal is increased [22]. McKay et al. [22] explained that by taking into account the mobility of the adsorbate (p-chlorophenol) molecules in a system where more particles was added, the turbulence from particles will be increased and possibly the effect of inter-particle shear reduces

Table 5
Intraparticle, pseudo-first and -second order kinetic parameters of MB adsorption onto diatomite at various masses of diatomite.

Mass of diatomite (g)	Pseudo-first order (Whole experimental data)			Pseudo-second order (Whole experimental data)			Intraparticle diffusion		External diffusion	Intraparticle diffusion		
	$q_{e,exp}$ (mg/g)	$q_{e,cal}$ (mg/g)	k_1 (1/min)	$q_{e,cal}$ (mg/g)	k_2 (g/mg min)	h (mg/g min)	k_p (mg/g $min^{1/2}$)	x_i	k_f (m/min)	k' (1/min)	D (cm^2/s)	R^2
1.7	101.1	9.874	0.0097	101.0	0.0072	73.46	1.98	86.71	0.022	0.2084	2.79×10^{-8}	0.8185
1.0	129.1	40.39	0.0025	106.4	0.0057	64.52	2.62	88.08	0.016	0.1296	1.73×10^{-8}	0.8964
0.7	180.6	69.02	0.0018	135.1	0.0049	89.49	3.98	106.6	0.018	0.0939	1.26×10^{-8}	0.8986
0.3	311.0	136.4	0.0023	232.6	0.0015	81.13	12.76	139.4	0.012	0.0672	8.99×10^{-9}	0.8744

the boundary layer to some extent. As a result, the mobility of the adsorbate will increase and possibly eases in crossing the boundary layer to the particle surface. It is also clear from the results reported in Table 5 that the calculated values of the adsorption capacity from pseudo-second order, $q_{e,cal}$, agree with the experimental value, $q_{e,exp}$, at 1.7 g. At lower weight, the $q_{e,cal}$ did not agree well. This may be explained by the formation of MB agglomeration on the diatomite surface.

4. Conclusion

It was clear that the adsorption MB onto diatomite was external diffusion controlled and in addition the adsorption processes obey the pseudo-second order process. The rate of adsorption of MB onto diatomite was very high in the first few minutes. This was then followed by a slower rate, and gradually approached a plateau. Equilibrium was reached after a rather long contact time of 50 min. The kinetics of adsorption of MB molecules onto diatomite was well represented by the pseudo-second order kinetic model. Various kinetic models were applied such as external and intraparticle diffusion models, which allow for investigating the important transport parameters such as the resistance of the external film and the diffusivity of the adsorption process. The experimental results suggest that the rate-limiting step mechanism of the adsorption of MB onto diatomite may vary throughout the adsorption process into different stages, (i) external diffusion which dominates at the beginning of the process (0–5 min), (ii) a reaction which might govern the subsequent part of the process (chemically adsorption), and (iii) intraparticle diffusion process, where the adsorption dramatically slows down.

References

[1] Z. Al-Qodah, Adsorption of dyes using shale oil ash, Water Research 34 (17) (2000) 4295–4303.
[2] M.A. Al-Ghouti, M.A.M. Khraisheh, S.J. Allen, M.N. Ahmad, The removal of dyes from textile wastewater: a study of the physical characteristics and adsorption mechanisms of diatomaceous earth, Journal of Environmental Management 69 (3) (2003) 229–238.
[3] C.W. Cheung, C.K. Chan, J.F. Porter, G. McKay, Elovich equation and modified second-order equation for sorption of cadmium ions onto bone char, Journal of Chemical Technology and Biotechnology 75 (2000) 963–970.
[4] C.W. Cheung, C.K. Chan, J.F. Porter, G. McKay, Film-pore diffusion control for batch sorption of cadmium ions from effluent onto bone char, Journal of Colloid and Interface Science 234 (2001) 328–336.
[5] Z. Aksu, G. Dönmez, A comparative study on the biosorption characteristics of some yeast for Remazol Blue reactive dye, Chemosphere 50 (2003) 1075–1083.
[6] M.A. Al-Ghouti, M.A.M. Khraisheh, S.J. Allen, M.N. Ahmad, Thermodynamic behaviour and the effect of temperature on the removal of dyes from aqueous solution using modified diatomite: a kinetic study, Journal of Colloid and Interface Science 287 (2005) 6–13.
[7] E. Guibal, C. Milot, J.M. Tobin, Metal-anion sorption by chitosan bead: equilibrium and kinetic studies, Industrial & Engineering Chemistry Research 37 (1998) 1454–1463.
[8] M. Hajjaji, S. Kacim, A. Alami, A. El Bouadili, M. El Mountassir, Chemical and mineralogical characterisation of a clay taken from the Moroccan meseta and a study of the interaction between its fine friction and methylene blue, Applied Clay Science 20 (2001) 1–12.
[9] M. Streat, J.W. Patrick, M.J. Camporro Perez, Sorption of phenol and para-chlorophenol from water using conventional and novel activated carbons, Water Research 29 (2) (1995) 467–472.
[10] D. Mohan, K.P. Singh, Single- and multi-component adsorption of cadmium and zinc using activated carbon derived from bagasse-an agricultural waste, Water Research 36 (2002) 2304–2318.
[11] M.M. Nassar, Intraparticle diffusion of basic red and basic yellow dyes on palm fruit bunch, Water Science and Technology 40 (7) (1999) 133–139.
[12] Y.S. Ho, G. McKay, Sorption of dyes and copper ions onto biosorbents, Process Biochemistry 38 (2003) 1047–1061.
[13] G.M. Walker, L. Hansen, J.A. Hanna, S.J. Allen, Kinetics of a reactive dye adsorption onto dolomitic sorbents, Water Research 37 (2003) 2081–2089.
[14] S.J. Allen, L.J. Whitten, M. Murray, O. Duggan, Adsorption of pollutants by peat, lignite, and activated chars, Journal of Chemical Technology and Biotechnology 68 (1997) 442–452.
[15] M.A.M. Khraisheh, M.A. Al-Ghouti, S.J. Allen, M.N. Ahmad, Effect of OH and silanol groups in the removal of dyes from aqueous solution using diatomite, Water Research 39 (2005) 922–932.
[16] K.A. Krishnan, T.S. Anirudhan, Removal of mercury(II) from aqueous solutions and chlor-alkli industrial effluent by steam activated and sulphurised activated carbons prepared from bagasse pith: kinetics and equilibrium studies, Journal of Hazardous Materials B92 (2002) 161–183.
[17] K.H. Chu, Removal of copper from aqueous solution by chitosan in prawn shell: adsorption equilibrium and kinetics, Journal of Hazardous Materials B90 (2002) 77–95.
[18] M. Jansson-Charrie, E. Guibal, J. Roussy, B. Delanghe, P.L. Cloirec, Vanadium(IV) sorption by chitosan: kinetics and equilibrium, Water Research 30 (2) (1996) 465–475.
[19] V.J.P. Poots, G. McKay, J.J. Healy, The removal of acid dye from effluent using natural adsorbent-I peat, Water Research 10 (1976) 1061–1066.
[20] V.J.P. Poots, G. McKay, J.J. Healy, The removal of acid dye from effluent using natural adsorbent., Wood, Water Research 10 (1976) 1067–1070.
[21] M. Korczak, J. Kurbiel, New mineral-carbon sorbent: mechanism and effectiveness of sorption, Water Research 23 (8) (1989) 937–946.
[22] G. McKay, M.J. Bino, A. Altememi, External mass transfer during the adsorption of various pollutants onto activated carbon, Water Research 20 (4) (1986) 435–442.
[23] C. Lee, K. Low, L. Chung, Removal of some organic dyes by hexane-extracted spent bleaching earth, Journal of Chemical Technology and Biotechnology 69 (1997) 93–99.
[24] J.R. Evans, W.G. Davids, J.D. MacRae, A. Amirbahman, Kinetics of cadmium uptake by chitosan-based crab shells, Water Research 36 (2002) 3219–3226.